Nanowire nonlinear plasmonics

Danveer Singh[a], G V Pavan Kumar[b*]

[a] *Photonics and Optical Nanoscopy Laboratory, Department of Physics and Department of Chemistry,*
Indian Institute of Science Education and Research (IISER), Pune 411008, India

[b] *Photonics and Optical Nanoscopy Laboratory, Department of Physics and Department of Chemistry,*
Indian Institute of Science Education and Research (IISER), Pune 411008, India

[*] *pavan@iiserpune.ac.in*

Nonlinear optics is one of the mature research fields relevant to fundamentals and applications of light-matter interaction. Several nonlinear optical processes such as second harmonic generation (SHG), two-photon resonances, four-wave mixing etc., have played critical role in realizing various optical devices. Plasmonic metals such gold and silver exhibit inherent non-linear optical behaviour. The nonlinear optical property of plasmonic nanostructures can be varied, modulated and eventually controlled by optimizing geometric features such as size, shape and arrangement of the nanostructures. One such plasmonic geometry that has captured attention in recent times is the plasmonic nanowire.

In this poster, we present non-linear optical microscopy studies performed on isolated plasmonic silver (Ag) nanowire architectures, especially in the context of second harmonic generation. First we studied a single isolated nanowire (150nm diameter, ~10 micron long) that was illuminated by femtosecond laser pulses (100fs and 80 MHz repetition rate) at various wavelengths through a high numerical objective lens (60x, 1.4 NA) and the back scattered light was collected and further processed. This back scattered light contained second harmonics (SH) and/or other nonlinear optical signals that were spatially mapped to the studied geometry. This spatial mapping method indicates the plasmonic hot-spot with excellent sensitivity and specificity. We further tested the efficiency of SHG signal as a function of excitation wavelength and found that the excitation spectral window was mainly confined to wavelengths close to twice the plasmonic resonance wavelength. Next we probed end-to-end coupled Ag nanowire-dimers, and found that the efficiency of SHG signal was greater at the nanowire junction compared to other location in the geometry. This enhanced SHG at the junction was facilitated by localized plasmon resonance at the nanowire-dimer junction. Such enhancement in the nonlinear optical processes due to geometrical coupling and tuning may find applications in plasmonic nano-cricuits and optical switching. Furthermore, such effects can also be enhanced by coupling the plasmonic nanowires with a gain-medium. We will discuss some of these prospects.

Enhancement of Fluorescence and Anisotropic Decay Dynamics from CdSe quantum dots by Hybrid photonic-Plasmonic template

S.R.K.Chaitanya Indukuri [1] and Jaydeep.K.Basu[1*]
Department of physics, Indian Institute of science,
Bangalore, 560012, India.
Email: basu@physics.iisc.ernet.in

The interaction between excitons and plasmons has generated a lot of interest and applications. The key aspect in studying the interaction is, in controlling the spatial distribution of exciton-plasmon sources. Self assembled block copolymer template (BCP) has an advantage of spatial control of both semiconductor quantum dots (SQD) and metal nano particles (MNP) to enable electromagnetic interaction between their excitations [1,2]. We are reporting optical studies on highly controlled placement of SQD in plasmonically active BCP template. Chemically synthesized CdSe quantum dot mixed with block copolymer solution was spin coated on glass and silicon substrates. Block copolymers can be self assembled in to hexagonal ordered cylindrical domains in the background matrix by spin coating. The lateral ordering is improved by solvent annealing. Effectively CdSe quantum dot prefers background matrix of the film. This material can act effectively like 2-D photonic slabs. The band gap is increased by the removing one block from the template making hexagonal ordered porous 2-D photonic slab.

To make this template plasmonically active we filled these pores with MNP using physical methods by varying the concentration of gold nanoparticles. Figure-1 shows the UV-Visible absorption spectrum of samples. Figure-2 shows room temperature Photoluminescence (PL) spectroscopy of these samples indicating enhancement of PL by local electric fields from metal nanoparticle antennas. Polarization dependent time resolved measurements show the anisotropic decay of CdSe quantum dot excitons. We explain these results with exciton-plasmon coupling and enhanced antenna effect of the MNP inside the photonic template and anisotropy in decay dynamics can be explained by the angle dependent reflectivity which gives change in the local density of states (LDOS) with different polarizations. These plasmonicaly active photonic templates can potentially be used as efficient bio-chemical sensors.

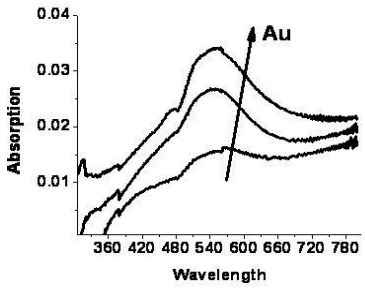

Figure 1: UV-Visible absorption spectrum of films with deferent MNP concentration inside the film

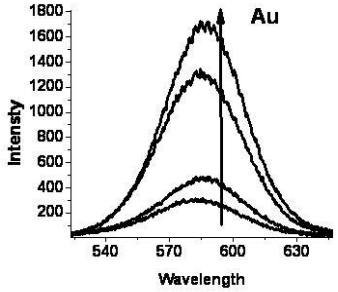

Figure 2: PL spectrum from samples with deferent concentration of MNP

Reference:
[1] M.Haridas, J.K.Basu, D.J.Gosztola and G.P.Wiederrecht, *Appl. Phys. Lett.*, **97**, 083307 (2010).
[2] M. Haridas, A. K. Tiwari, M. Venkatapathi , J. K. Basu *J. Appl. Phys.*, (2013-in press).

Energy-Momentum Spectroscopy of Plasmonic Metamaterials

Ravi PN Tripathi, Rohit Chikkaraddy, Arindam Dasgupta, G.V.Pavan Kumar*
**Photonics and Optical Nanoscopy Laboratory, Department of Physics and Chemistry*
**Indian Institute of Science Education and Research, Pune- 411008, India*
*pavan@iiserpune.ac.in

Metamaterials are artificially fabricated structures, which lead to unconventional optical properties which are otherwise difficult to achieve using conventional materials. One of the interesting categories of metamaterials is made of plasmonic metal such as gold and silver. Such metamatrials with plasmonic constituents have led to interesting applications such as lenses with sub-wavelength optical resolution, ultra-sensitive optical antennas, optical cloaks etc. Since; the optical properties of such metamaterials have a strong dependence on shape, size and periodicity of individual plasmonic, therefore, it is important to probe the optical response in energy and momentum space. In this poster, we will emphasis on energy- and momentum- resolved optical spectroscopy technique that we are developing to characterize plasmonic metamaterials.

The energy-momentum spectroscopy provides an effective way to study elastic and inelastic light-material interactions down to the level of nanoscale, and can effectively probe how optical properties change with symmetry and arrangement of the structure. Furthermore, this spectroscopy method can also be employed to study single-emitters interacting with plasmonic metamaterials on surface or embedded beneath it. The developed methodologies can be extrapolated to probe gain-assisted plasmonic response and plasmonic hot-spot on two dimensional surface.

Aligned ITO nano-structured electrodes for organic photovoltaics

Arun D Rao[a], Jhuma Dutta[b], S.A. Ramakrishna[b] Praveen C Ramamurthy[a,*]
[a] *Indian Institute of Science, Bangalore, Karnataka, 560012, India*
[b] *Indian Institute of Technology, Kanpur, 208016, India*
* *praveen@materials.iisc.ernet.in*

Vertically aligned columns of indium tin oxide (ITO) on a glass substrate were used for fabricating organic photovoltaic device(OPVD). ITO structures were fabricated by e-beam evaporation technique. Nanostructured columns form direct paths for charge transport by creating high surface area. High surface area nanostructured ITO enhance charge collection of the active layer. Here, devices with aligned ITO columnar structure OPVD showed three fold increases in current density compared to the planar structured ITO. Hence there is significant increase in photovoltaic performance.

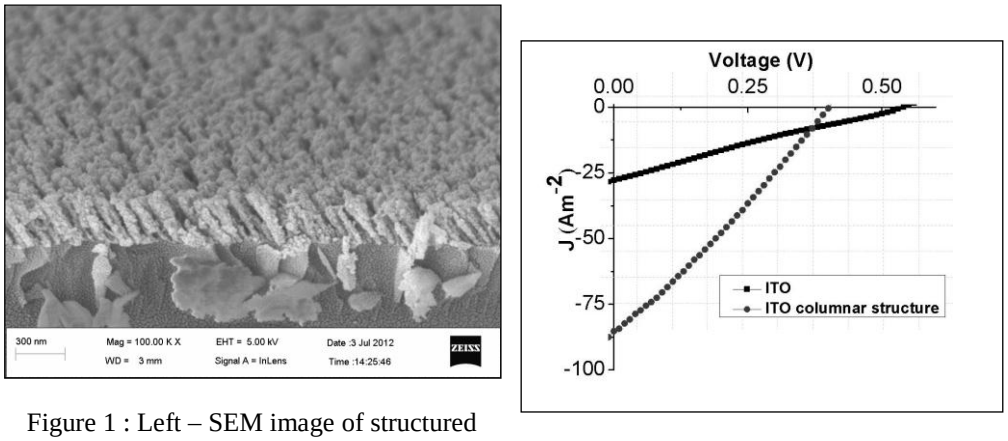

Figure 1 : Left – SEM image of structured ITO, Right – J-V characteristics of OPV with structured and controlled ITO [1]

References:

[1] Jhuma Dutta, S.A. Ramakrishna and A. Lakhtakia, *Blazed gratings of periodically patterned columnar thin films,* Appl. Phys. Lett. **102**, Art. No. 161116 (2013)

\

Energy-Momentum Spectroscopy of Plasmonic Metamaterials

Ravi PN Tripathi, Rohit Chikkaraddy, Arindam Dasgupta, G.V.Pavan Kumar*
**Photonics and Optical Nanoscopy Laboratory, Department of Physics and Chemistry*
**Indian Institute of Science Education and Research, Pune- 411008, India*
*pavan@iiserpune.ac.in

Metamaterials are artificially fabricated structures, which lead to unconventional optical properties which are otherwise difficult to achieve using conventional materials. One of the interesting categories of metamaterials is made of plasmonic metal such as gold and silver. Such metamatrials with plasmonic constituents have led to interesting applications such as lenses with sub-wavelength optical resolution, ultrasensitive optical antennas, optical cloaks etc. Since; the optical properties of such metamaterials have a strong dependence on shape, size and periodicity of individual plasmonic, therefore, it is important to probe the
optical response in energy and momentum space. In this poster, we will emphasis on energy- and momentumresolved optical spectroscopy technique that we are developing to characterize plasmonic metamaterials.

The energy-momentum spectroscopy provides an effective way to study elastic and inelastic lightmaterial interactions down to the level of nanoscale, and can effectively probe how optical properties change with symmetry and arrangement of the structure. Furthermore, this spectroscopy method can also be employed to study single-emitters interacting with plasmonic metamaterials on surface or embedded beneath it. The developed methodologies can be extrapolated to probe gain-assisted plasmonic response and plasmonic hot-spot on two dimensional surface.

Inorganic-organic hybrid semiconductors: Fabrication and optoelectronic applications

Shahab Ahmad and G. Vijaya Prakash*
Nanophotonics Lab, Department of Physics, Indian Institute of Technology Delhi, Hauz khas, New Delhi 110016, India
* *prakash@physics.iitd.ac.in*

Inorganic-Organic (IO) hybrid semiconductors have emerged as a class of novel materials over the last two decades, as they combine distinct and diverse functionalities into a unique material through various chemical or physical interactions. These materials demonstrated potential advantages nearly everywhere: photonics, optoelectronics, solar cells, sensors and biology. IO hybrids of type $(R\text{-}NH_3)_2MX_4$ (R=organic, M = divalent Metal and X=halogen), have been a special focus because of their self-organized natural quantum well type structures, consisting of alternatively stacked up MX_4^{2-} semiconductor and organic insulator quantum sized layers. Owing to their large exciton binding energy induced by dielectric and quantum confinement effects, these material exhibits pronounced room-temperature optical (Mott type) excitons [1-3].

These hybrids can be considered as designer materials, since the exciton properties can be conveniently tailored, depending on the constituent metal and halide ions. For example, in $(R\text{-}NH_3)_2PbI_{4(1-y)}Br_y$ (y=0-1) mixed IO-hybrid system, the emission can be tuned over a wide range, from 520 to 390nm, from selective replacement of I with Br atom. Strong room-temperature excitonic features, relatively high thermal durability and newly developed intercalation fabrication method for device quality films prompted us to explore applications such as exciton based IO-LEDs and IO photo-detectors [2-5]. The results will be discussed in detail.

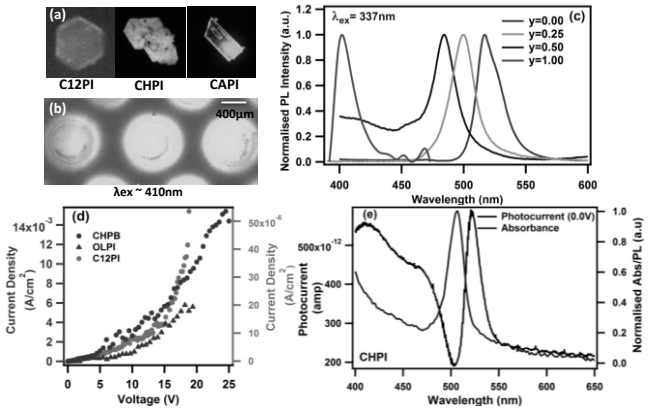

Fig.1: These IO hybrid semiconductors demonstrates the ability for (a) strong-room temperature exciton emission, (b) device quality photonic structures (c) wide range of emission tenability, (d) strong ability for the development of IO-LEDs and (e) strong exciton related photocurrent leading to exciton photo-detectors.

References:

[1] D. B. Mitzi, C. A. Field, W. T. A. Harrison and A. M. Guloy, *Nature (London)* **369**, 467 (1994)
[2] K. Pradeesh, J. J. Baumberg and G. Vijaya Prakash, *Opt. Express* **17**(24), 22171 (2009); Appl. Phys. Lett. 95, 033309 (2009);); Appl. Phys. Lett. 95, 173305 (2009).
[3] K. Pradeesh, K.N. Rao and G. Vijaya Prakash, *J. Appl. Phys.*. **113**, 083523 (2013)
[4] K. Pradeesh, and G. Vijaya Prakash, *J. NanoSci.NanoTech.* **11**, 10715 (2011).
[5]I. Saikumar, Shahab Ahmad, J. J. Baumberg and G.Vijaya Prakash, *Scripta Mater.* **67**, 834 (2012)

PT-symmetric Quadrimer: Closed-form structure

Samit Kumar Gupta*, Amarendra K. Sarma
Indian Institute of Technology Guwahati, Guwahati-781039, Assam, India.
*Email: samit.gupta@iitg.ernet.in

In recent times, there have been growing interests in the field of Parity-time (PT) symmetric systems both theoretically and experimentally, due to its immense potential applications in diverse areas of interests. In the pioneering work of Bender et al [1], it was shown explicitly that even if the Hamiltonian is non-Hermitian, conditionally it can yields entirely real spectra. Later on, in their path-breaking work of [2], Christodoulides and co-workers implemented the concepts of PT-symmetry in Optics in a coupled two-waveguides (WG) system. We attempt to devise the framework for realizing PT-synthetic materials for useful applications.

In our work, we are considering four coupled waveguides system as shown in Fig. (1).

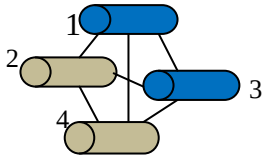

Fig. 1: Schematic of the Quadrimer system. Here WG1, WG3 are having gain and WG2, WG4 are having loss.

The Hamiltonian of the system in the linear regime and without considering couplings between WG1 $\leftrightarrow$ WG4 and WG2 $\leftrightarrow$ WG3 is

$$H = \begin{bmatrix} ig & -\kappa_{12} & -\kappa_{13} & 0 \\ -\kappa_{12} & -ig & 0 & -\kappa_{24} \\ -\kappa_{13} & 0 & ig & -\kappa_{34} \\ 0 & -\kappa_{24} & -\kappa_{34} & -ig \end{bmatrix} \quad (1)$$

where, ‘g’ is the gain/loss coefficient, κ_{ij} are the coupling constants between waveguides i and j.

From equation (1), we find that the system is PT-symmetric under the condition: $\kappa_{12} = \kappa_{34} (= \kappa$ say) and $\kappa_{13} = \kappa_{24} (= \alpha,$ say). Interestingly, we also find that the inclusion of the couplings between WG1 $\leftrightarrow$ WG4 and WG2 $\leftrightarrow$ WG3 do not disturb the PT-symmetry of the system. The eigen-values are obtained as: $\gamma \pm \sqrt{\kappa^2 - g^2}$, $-\gamma \pm \sqrt{\kappa^2 - g^2}$. It could be seen that the PT-symmetry threshold point or exceptional point is $g_{th} = \kappa$, which is exactly same as in the dimer case [2]. We have investigated the eigen-modes of the system below and above the threshold point. We find that some of the eigen-modes below and above the PT-threshold coalesce at the exceptional point.

The beam propagation dynamics of the system is also investigated in both the linear and the nonlinear regimes. In the linear regime, below the threshold, we observe non-reciprocal power oscillations in the waveguides due to real eigen-values of the system. On the other hand, above the threshold, we observe powers increasing in the gain-guides in an exponential manner owing to imaginary eigen-values (non-reciprocal). In nonlinear case, we observe diminution in power oscillations and asymmetrical response. We have also studied the ladder-like open-form structure reducible from this closed-form scheme and find exact congruency.

References:

[1] C. M. Bender, S. Boettcher, Phys.Rev.Lett. **80**, 5243-5246 (1998).
[2] C.E. Ruter et al, Nature Physics, **6**, 192-195 (2010).

Fluorescent gold nanoparticles: as a platform for visual urea sensing

Upendra Kumar Parashar[a,c,*], N. R. Nirala[b], P. S. Saxena and Anchal Srivatava[c]
[a] *Department of Physics, Indian Institute of Technology, Kanpur-208016, India*
[b] *Department of Zoology, Banaras Hindu University, Varanasi-221005, India*
[c] *Department of Physics, Banaras Hindu University, Varanasi-221005, India*
* *upendra@iitk.ac.in*

The surface plasmon band (SPB) maxima shift phenomenon is the main key in molecular sensing done so far employing gold nanoparticles (Au-NPs) as a substrate. Gold nanoparticles are very popular as substrate for sensing applications due to their suitability for various kind surface modifications with a variety of functional groups using thiol chemistry.

Here, we report a surfactant free synthesis of mono-disperse gold nanoparticles, their functionalization and utilization of these gold nanoparticles for visual sensing of urea in aqueous medium. To develop this technique we have modified the surface of the gold nanoparticles with some functional moieties and immobilized the urease enzyme on these functionalized gold nanoparticles using carbodiimide chemistry. The anchoring of urea on the surface of urease immobilized gold nanoparticles resulted the change in the surface morphology, which leads to the change in its optical properties and finally, leads to the color change of the colloidal suspension. The lower detection limits govern by the shift in SPB maxima and fluorescence quenching was found about 2 mg/dL and 3mg/dL respectively. In brief, the urea detection approach reported here is simple, one step process and applicable on field, which is specifically important for the population, where the higher end diagnostic techniques are unaffordable or inaccessible.

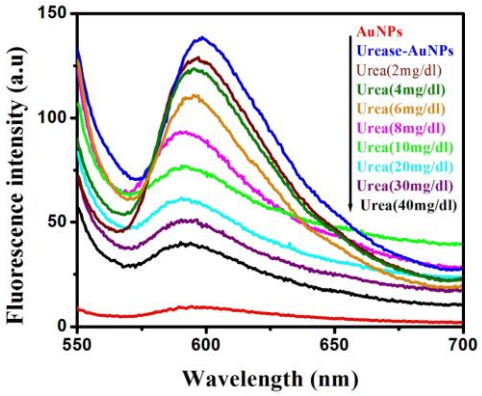

References:

[1] M. C. Daniel, D. Astruc, *Chem. Rev.*, **104**, 293-346 (2004).
[2] S. Eustis, M. A. El-Sayed, *Chemical Society Reviews*, **35**, 209-217 (2006)
[3] N. Nath, A. Chilkoti, *Analytical Chemistry*, **74**, 504-509 (2001)

Photonic structures of mixed semiconductors from self-assembled templates

Suman Shakya1[a] and G.Vijaya Prakash2[a]*

[a]*Nanophotonics Lab, Department of Physics, Indian Institute of Technology Delhi, Hauz Khas, New Delhi 110016, India*

[*]*Email: prakash@physics.iitd.ac.in*

Abstract: In the present abstract we have prepared 2D photonic crystals template [1] and interstitial space is filled by varying stoichiometry of $CdSe_xTe_{1-x}$ with the help of Electro-chemical deposition technique after optimizing the deposition parameters[2]. Subsequently, the polymer spheres were removed using appropriate organic solvents, resulting in inverted voids as perfect replica of the spheres also know as inverse opal structure[3]. Schematic diagram of fabricated template structure by this process is shown in figure 1a. Electrodeposition also gives opportunity to modify crystalline nature of micro/mesa structure by varying electrodeposition parameters. Stoichiometry of the film can be controlled and thereby band gap tuning is possible in this technique. Figure 1(b) & 1(c), shows the 2D photonic structure of $CdSe_xTe_{1-x}$ and 2D polymerspheres template respectively.

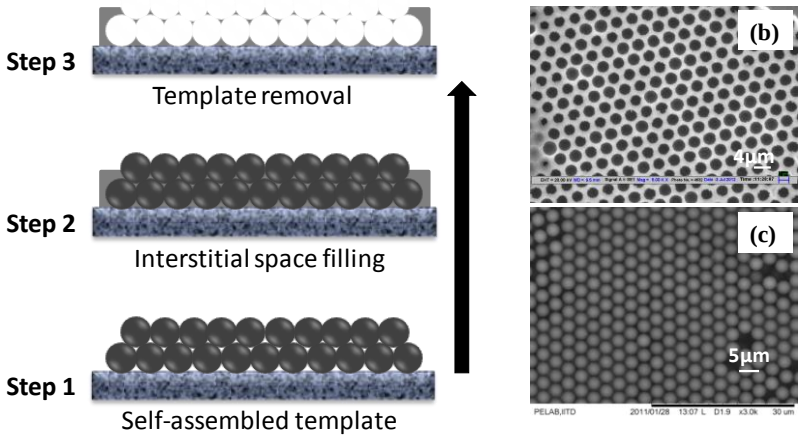

Fig. 1(a) Schematic showing the process of fabrication, (b) $CdSe_xTe_{1-x}$ photonic structure after the removal of polymerspheres (c) SEM image of polymerspheres templates(3µm).

References:

[1] Juan F. Galisteo-Lopez, Marta Ibisate, Riccardo Sapienza, Adv. Mater. **23**, 30-39 (2011)

[2] G. Vijaya Prakash, Rahul Singh, Ashwani Kumar, Mater. Lett. **60,** 1744–1747 (2006)

[3] K.Pradeesh, Nageswara Rao Kotla, Shahab Ahmad, G.Vijaya Prakash, Journal of Nanoparticles **531871**,13 (2013)

Anisotropic diffraction from oblique columnar Ag thin films on DVD grating templates

Pratibha Goel*, Kalpana Singh Solanki, J. P. Singh
Department of Physics, Indian Institute of Technology Delhi, New Delhi-110016, India
**pratibha.goel@physics.iitd.ac.in*

The s- and p- polarization diffraction spectra of Ag nanorods arrays prepared on DVD-R by oblique angle deposition are studied in detail. Diffraction induced surface plasmon excitation can produce enhanced transmission at selected position of the visible spectra. The change in the diffraction spectra as a function of nanorods length can be used to track the growth dynamics of the nanorods [1]. SEM images of bare DVD-R template and Ag columnar thin film are shown in Fig 1 (a) and (b) respectively. A color diffraction image of bare DVD-R (Fig. 1(b)) exhibits three dominant features; a white circular spot at the center which represents the light transmitted directly through the sample referred as 0^{th} order and two elliptical spots which were observed on right and left sides of the central spot referred as +1 (right) and -1 (left) diffracted order. It is worth noting that the diffraction image is independent of polarization in case of bare DVD-R (Fig. 2) whereas the columnar Ag films on DVD-R show a significant difference between s- and p-polarized diffraction spectra (Fig. 3). With increase in film thickness, 0^{th} order peak gets attenuated in both the cases due to the absorption. The anisotropic morphology of the columnar Ag film results into an anisotropy in the +1 and -1 diffraction orders. This anisotropy in the morphology is caused by the shadowing effect during oblique angle deposition. For p-polarized diffraction spectra, some additional features such as strong transmission in +1 diffracted order were also observed. This may be due to the excitation of the surface plasmon at the Ag/air interface of the DVD grating template.

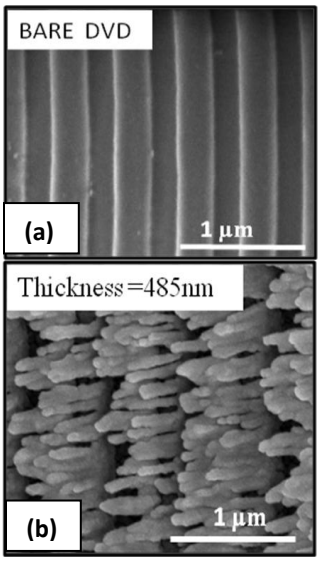

Fig. 1: *SEM image of (a) bare DVD, and (b) Ag nanorods respectively*

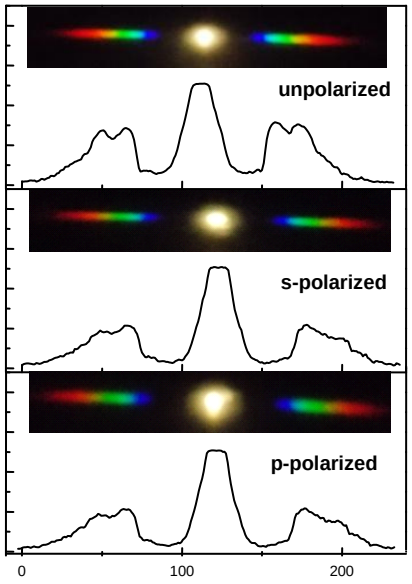

Fig. 2: *Diffraction pattern and corresponding line profile of bare DVD with unpolarized, s-polarized and p-polarized light*

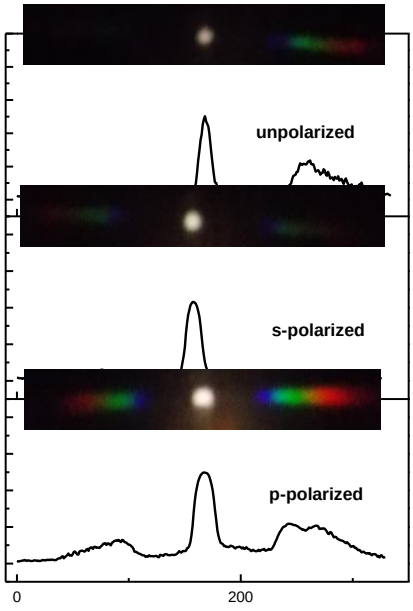

Fig. 3: *Diffraction pattern and corresponding line profile of Ag nanorods grown DVD with unpolarized, s-polarized and p-polarized light*

References:

[1] W. H. Yeh, J. W. Petefish, and A. C. Hillier, *Anal. Chem.* **83**, 6047 (2011)

A Compact Metamaterial Unit Cell based T Power Divider for Ku band Applications

Abhishek Shukla[1], Dr. K. K. Sood[2] and Rajeev Jyoti[3]
[#]1, 2,3 *Antenna Systems Group, Space Applications Centre, India*
abhisheks@sac.isro.gov.in

Abstract - Properties of a Metamaterial[MTM] CRLH[Composite Right-Left Hand] based T Power dividers working at Ku band are investigated , based on unit cell parameters. Micro strip gaps and via holes whose behavior is equivalent to the combination of series capacitors and shunt inductors respectively, that is, a dual TL (high-pass) configuration is important element of the metamaterial unit cell. Characteristics of the Metamaterial-medium can be set to achieve a desired phase shift by adjusting the parameters of these structures. A 50% reduction of the length of the impedance transformer, without significant RF performance degradation, has been achieved. The phenomena are demonstrated by simulated and measured results. Proposed power divider is very suitable for microwave and millimeter wave integrated circuits because of compact in size and low-cost.

Introduction -

Power Dividers play an important role in almost any RF and microwave communication system because of their ability to divide power [4]. Different types of Power dividers exist [4]. These power dividers are used in the design of power amplifiers, antenna arrays to split the RF signal, and other RF applications. Conventional Radial power dividers use a multiple of λ/2 (90°) line between the center feeding line and the output ports. This λ/2 length provides an opened circuit when terminated with an opened circuit but the physical length of these multiple of λ/4 (90°) lines can occupy a large area on RF boards. However by using MTM it is possible to design lines with an electrical length of 0° for a single band operation with minimum losses [5, 6]. This zero degree property is accomplished by taking advantage of the interesting MTM properties, such as anti-parallel phase/group velocity, nonlinear phase slope and positive phase offset at DC.

This paper discusses about the MTM Power dividers using this combination of CRLH based unit cell approach. A parametric study has been done also showing its various critical design parameters, achieving a required amount of phase shift and RF performances. This Power divider exhibits similar power splitting characteristics as the "conventional "while it leads to major (significant size reduction of dimension of Matching Section with respect to Conventional Power divider).

Electrically Small Metamaterial Antennas on Flexible Substrate

Vaishali Rawat and Sangeeta.N.Kale*
Defence Institute of Advanced Technology, Pune
* sangeetakale@diat.ac.in

Metamaterial[1, 2,] and Flexible electronics[3, 4] are the current state of the art research fields of this century. In our work, we have made an effort to amalgamate these two areas. We have designed a prototype metamaterial antenna[5, 6, 7] on a flexible substrate[8].

The antenna is modelled using a polyimide substrate (ϵ =3.5) which has the advantages of being lightweight, flexible, and resistant to heat and chemical reactions. The antenna is designed at 4.56 GHz as this frequency has space and defence applications. The simulations are carried out in CST Microwave Studio.

Firstly, we have designed a unit cell of Split Ring Resonator (SRR) [9] structure which gives resonance at 4.6 GHz. Further, we have designed a conventional circular patch antenna on polyimide substrate at 4.56GHz. Thereafter, we used SRR as the substrate and designed the antenna at same frequency. Comparsion between conventional antenna and metamaterial antenna are done in Table 1.It is clearly envisioned that MM antenna has size much smaller than the conventional antenna size with equal return loss. Figure 1 depicts the simulated return loss of polyimide and metamaterial antenna.

Table 1: Comparison between polyimide and metamaterial antenna in regard of dimensions

Description	Polyimide(mm)	Metamaterial(mm)
Radius	16	7
Substrate Width and Length	60	20
Transmission line Width	0.84	0.84
Transmission line Length	12	4

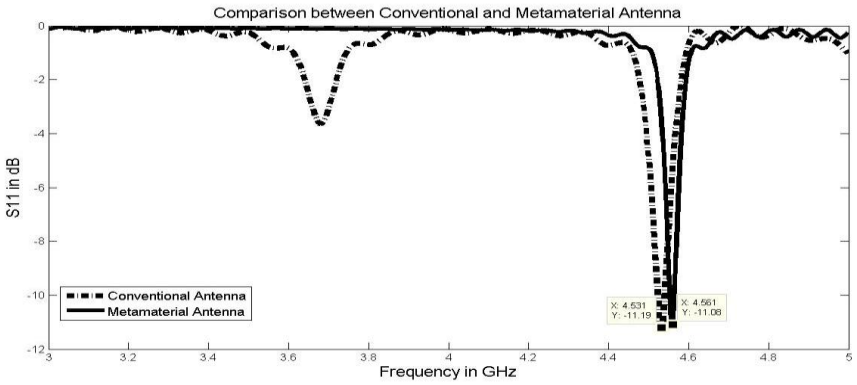

Figure 1: Return loss of polyimide and metamaterial antenna

References:

[1] R. A. Shelby, D. R. Smith, S. Schultz, Science, **292**, 77 (2001)
[2] R. A. Shelby, D. R. Smith, S. C. Nemat-Nasser, and S. Schultz, *App.Phy. Lett.* **78**, 489 (2001)
[3] Arokia Nathan et.al. *Proceedings of the IEEE*, **100**, 1486 (2012)
[4] http://en.wikipedia.org/wiki/Flexible_electronics
[5] Filiberto Bilotti, Andrea Alù, Nader Engheta, and Lucio Vegni, *Proc.EuCAP* (2006)
[6] M.Z.M.Zani, M. H. Jusoh, A. A. Sulaiman, Baba, R. A. Awang, M. F. Ain, *IEEE* ICDESA (2010)
[7] Saman Jahani, Jalil Rashed-Mohassel, Mahmoud Shahabadi, *IEEE Trans. Antennas and Wireless Propag*, **9**, 1194(2010)
[8] In Kwang Kim and Vasundara V. Varadan, *IEEE*, *10*, 3333 (2010)
[9] J. B. Pendry et al., *IEEE Trans. Microwave Theory Tech*., 47, 2075 (1999)

Fabrication of butt-coupled cantilever waveguide by FIB milling on MEMS SOI beams

Prem P. Singh[1*], C. Venkatesh[2], RenilKumar[1], Manoj Varma[1] and Rudra Pratap[1]

[1]*Centre for Nano Science and Engineering, Indian Institute of Science, Bangalore-560012, India*

[2] *School of Electrical, Electronics and Computer Engineering, The University of Western Australia, Crawley -6009, Australia*

* premnano@mecheng.iisc.ernet.in

In the last few decades, MEMS based micro-cantilevers have been extensively explored for application in the field of chemical and bio sensing, owing to their high sensitivity, small form factor and mass fabrication capabilities. Another advantage of this technology is its large multiplexing capability, which provides a means for the realization of multi-analyte sensor array platform by functionalizing each cantilever with differential receptors. The mode of sensing in such sensors can be either static or dynamic depending on measured structural deformations or change in resonance frequency. Combining micromachining technology with guided wave optics opens up a new extension of MEMS called Optical MEMS (MOEMS) that offers immense potential for sensing applications. Binding of any external agent on cantilever waveguide deforms it, which can be measured from the change in the coupled output optical power. Silicon-on-insulator platform is an ideal choice for photonics waveguide applications due to the high refractive index contrast and has been chosen for this work.

We present a fabrication process and realization of 200 nm thick SOI based fixed-fixed silicon beams to be used as optical waveguides for sensing applications. The waveguide cantilevers separated by a small gap of a few hundred nanometers have been realized by cutting a released fixed-fixed beam at the center using Focused Ion beam (FIB). To reduce the stress build up on the cantilever during the milling process [1], a combination of high beam current and low ion beam energy is used. Figures 1 and 2 depict the suspended fixed-fixed beam on SOI platform and the cantilevers realized by cutting the beam at the center respectively.

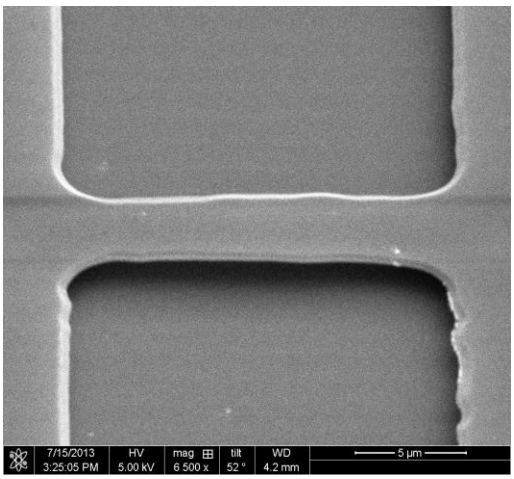

Fig1. Fabricated SOI based Si beams

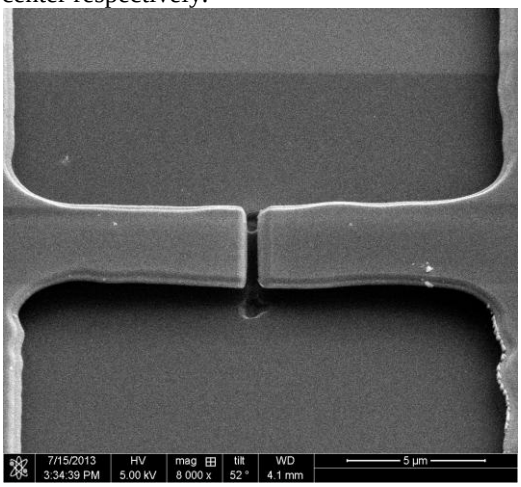

Fig.2. Fabrication of coupled cantilever waveguide

References:

[1] C. Venkatesh, Prem P. Singh *et. al*, "Effect of FIB milling on MEMS SOI cantilevers", Proc. Conference on Optoelectronics and Microelectronics Materials & Devices (COMMAD), Melbourne *(2012),* DOI: 10.1109/COMMAD.2012.6472412

Propagation lengths of fundamental surface plasmon mode in silver nanowires

Jitender*, R. K. Varshney and Arun Kumar
Department of Physics, Indian Institute of Technology Delhi, New Delhi-110016
* jitender@physics.iitd.ac.in

Surface plasmons are the electromagnetic waves coupled with electronic oscillations at the metal-dielectric interfaces. Nano range confinement of surface plasmons has found potential applications in miniaturized photonic circuits. It has been reported widely in the literature that Ag nanowires have excellent properties[1] to be used in the various applications such as in photonic circuits, sensors, resonators[2] and interconnects etc. One of the most important properties for these applications is the propagation length of the surface Plasmon wave.

In this study, we have calculated propagation lengths of the fundamental surface plasmon mode of silver nanowires with different radii embedded in a silica matrix, as a function of wavelength using both analytical method as well as standard software (COMSOL 4.3b). The schematic of the structure used for the simulation is shown in Fig. 1. The nanowire is immersed in a uniform silica matrix with refractive index n_1=1.45. We have used Jhonson & Cristy data [3] for permittivity of silver nano-wire. For our analytical calculations, complex propagation constant of the surface Plasmon mode is obtained by solving the following equation

$$\frac{K_l'(\gamma_m a)}{K_l(\gamma_m a)} - \frac{\varepsilon_m \gamma_m I_l'(ka)}{\varepsilon_1 I_l(ka)} = 0; \quad \gamma_m = \sqrt{\beta^2 - \omega^2 \mu \varepsilon_1} \text{ and } k = \sqrt{\beta^2 - \omega^2 \mu \varepsilon_m} \qquad (1)$$

In the above equation the symbols have their usual meanings

Results obtained from both the approaches mentioned above are found to be matching. Figure 2 shows the variation of propagation length for different nanowires as a function of wavelength. The figure shows that the propagation length increases with increase in the radius and in all the cases it has a sharp peak at wavelength 1080 nm. So it is clear that 1080 nm is the wavelength to be used for applications needing large propagation lengths.

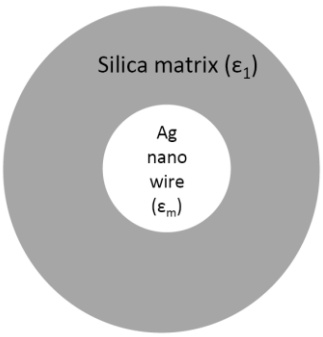

Fig. 1. Cross-section of structure having Ag nanowire in silica matrix

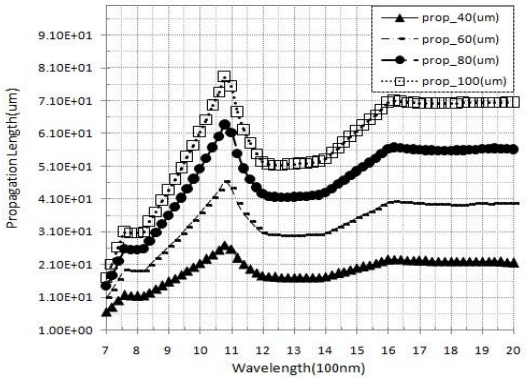

Fig. 2. Variation of Propagation length with wavelength for nanowires of different radii.

References:

[1] B. Wild, L. Cao, Y. Sun, B. P. Khanal, E. R. Zubarev, S. K. Gray, N. F. Scherer, and M. Pelton, ACS Nano **6**(1), 472–482 (2012).

[2] H. Ditlbacher, A. Hohenau, D. Wagner, U. Kreibig, M. Rogers, F. Hofer, F. R. Aussenegg, and J. R. Krenn, Phys. Rev. Lett. **95**(25), 257403 (2005).

[3] P. B. Johnson and R. W. Christy Phys. Rev. B **6**(12), 4370–4379(1972).

Compact wavelength division multiplexer using nonlinear polystyrene cavities in 2D photonic crystal structure

Pankaj K Sahoo and Joby Joseph
Photonics Research lab, Department of Physics, Indian Institute of Technology Delhi, New Delhi, India 110016
8pankaj8@gmail.com

We present here a compact wavelength division multiplexer (WDM) employing the intensity dependent behavior of Polystyrene (PS). PS is a nonlinear organic conjugated polymer with linear refractive index of 1.59. It has a large 3rd order nonlinear susceptibility of the order of 10^{-12} cm^2/W and fast response time of the order of femtoseconds [2]. This large nonlinearity arises due to the delocalization of π -conjugated electrons along the polymer chain. Our WDM (Fig. 1a) is a 2D PhC consisting of square lattice of silicon rods (r.i. =3.4, r=1.8*a*, *a* being the lattice constant) in air with three output waveguides, each coupled to a cavity. The central cavity is symmetric & linear. The two outer cavities are made asymmetric by inserting elliptical PS rod of optimized axis lengths 0.48*a* & 0.56*a* along the x & y axes respectively, which have two different resonance frequencies (normalized) w_x=0.4067 & w_y=0.3855 along x & y axes respectively. These cavities are coupled to a common coupler region, which is an empty region without Si rods. It connects the three cavities to the input waveguide. A control signal is applied to the two outer cavities through separate waveguides (left & right).

The frequency of the control signal is chosen as the resonance frequency of the cavity along X-direction i.e., w_x = 0.4067 (λ = 1.55 μm for *a* = 0.63 μm), so that it doesn't couple to y-direction to avoid crosstalk between input and control signal. When the intensity I of control signal increases, the r.i. of the material (PS) of the two outer cavities increases due to nonlinear effect ($\Delta n = n_2 I$). As a result the output frequency w_y of the outer cavities shifts downward. The amount of shift depends on the intensity of control signal. So we will get a dynamic WDM whose output wavelength is optically controlled. Fig. 1 (b) shows the plot of transmittance vs. normalized frequency for central cavity. The output frequency of central cavity (=0.386132265) is fixed as it is not nonlinear. Fig. 1 (c) shows the transmittance plot for the two outer cavities. Since the outer two cavities are symmetric w.r.t the coupler region both have same transmittance characteristics. The output frequencies corresponding to three intensities I_1, I_2, I_3 ($I_1 > I_2 > I_3$) are 0.3856, 0.3853, and 0.3852 respectively.

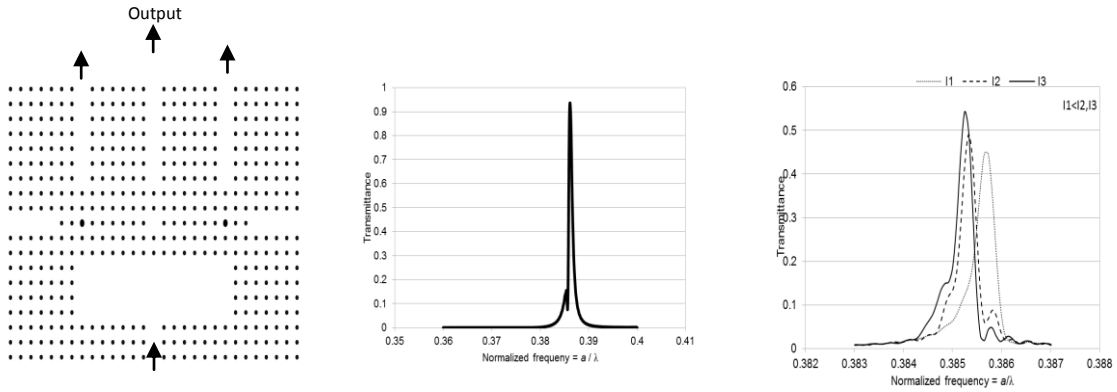

Fig.1: (a) WDM (b) Transmittance of central cavity (c) Transmittance of left & right cavity

References:

[1] V Liu & Y Jiao, D Miller & S Fan, *Optics Letters* **36**, 591 (2011).
[2] Ye Liu, Fei Qin, Zhi-Yi Wei, Qing-Bo Meng, Dao-Zhong Zhang and Zhi-Yuan L, Appl. Phys. Lett. **95**, 131116 (2009).

Angle-dependant Goos-Hanchen shift from glass-Ag interface

Dipak Rout,* Raj Kishen R.K. and R.Vijaya
Department of Physics, Indian Institute of Technology Kanpur, Kanpur 208016, India
** dkrout@iitk.ac.in*

The Goos-Hanchen (GH) shift is the lateral shift of the point of reflection of a beam of light during total internal reflection, at angles close to the critical angle [1]. This shift is usually very small and difficult to detect at the interface between two dielectrics. Here, we experimentally demonstrate relatively large positive and negative shifts aided by the plasmonic effect of evanescent wave enhancement during a single reflection from the chosen interface. As shown in Fig. 1(a), light at a wavelength λ of 632.8 nm from a *CW* He-Ne laser is incident on a glass prism of refractive index 1.43. The critical angle for the glass-air interface is thus 44.37^0. A thin film of silver (Ag) of refractive index $0.13+3.99i$ is deposited as a strip of 4mm width on the back side of the prism. A position-sensitive photo-detector (PSPD) and an oscilloscope in X-Y mode (DSO) are used to record any shift in the beam position. The GH shift is measured by changing parameters such as the angle of incidence of light (ϕ), point of incidence (x) on the metal film, the state of linearly polarized light and different thicknesses of the Ag film.

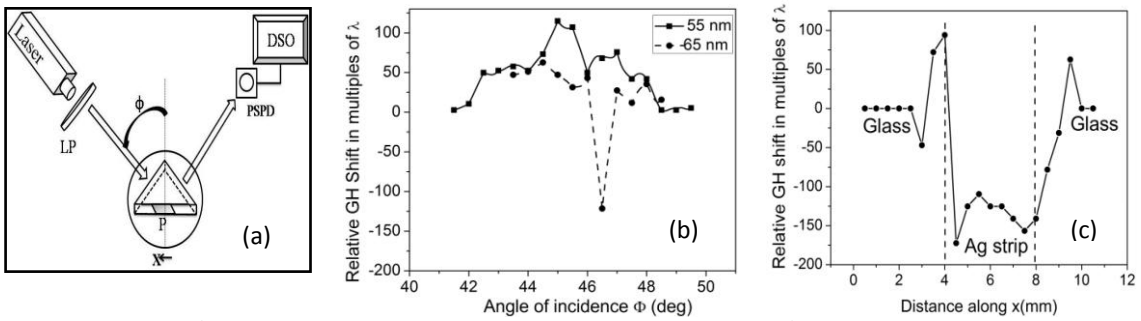

Fig.1 (a) Schematic of the experimental set up with linear polarizer (LP), prism with Ag film on the base (P), position-sensitive photo-detector (PSPD) and an oscilloscope acquiring data in X-Y mode (DSO), (b) angle dependence of relative GH shift shown for two different Ag film thicknesses and (c) relative GH shift measured at different positions across the base of the prism, at an incident angle of 46.5^0 for a film thickness of 65 nm, with dashed vertical lines representing the location of the Ag film of 4mm width.

At the critical angle, there is no plasmonic enhancement for *s* polarisation [2]. However, small fluctuations due to mechanical movements are unavoidable in the measurements. Hence, the *relative* GH shifts (in multiples of wavelength λ) between the *p* and *s* polarized light measured for two different thicknesses of Ag film are shown in Fig. 1(b). Each data point is the average of several measurements. A clear observation of a large negative shift at an angle of 46.5^0, close to the expected angle for matched plasmon-photon wave vector condition, is obtained for a film thickness of 65nm due to the contribution from the surface plasmons excited at the interface between air and the absorbing Ag film [3]. For film thicknesses above a certain critical value, the shift is negative as reported in [2]. In Fig. 1(c), the GH shift for the film thickness of 65 nm is shown while scanning along the base of the prism, which reinforces the large shift seen in Fig. 1(b). The largest absolute negative shift observed is 101 μm, which is equivalent to 160λ. The smallest shift that can be measured unambiguously is 6 μm (10λ) in this arrangement.

The present work can be extended to the study of photonic nanostructures, wherein the shift is expected to be higher near the stop-band edges in the presence of strongly evanescent modes. In addition, photonic structures infiltrated with metal nanoparticles may show even larger GH shifts than dielectric structures due to the excitation of plasmonic modes.

References:

[1] Xuanbin Liu, Zhuangqi Cao, Pengfei Zhu, Qishun Shen and Xiangmin Liu, *Phys. Rev.E* ,73, 056617 (2006).
[2] X. Yin, L. Hesselink, Z. Liu, N. Fang and X. Zhang, *Appl. Phys. Lett.* **85**, 3 (2004).
[3] S. Ghosh, K. Brahmachari and M. Ray, *Journal of Sensor Technology*, **2**, 48 (2012).

Enhancing birefringence of suspended core photonic crystal fiber by selectively filling air holes with metal-wire

Tushar Biswas[a], Surajit Bose [a], Mrinmay Pal[a], and Shyamal K Bhadra[a,*]
[a] *Fiber Optics and Photonics Division, CSIR-Central Glass and Ceramic Research Institute, 196 Raja S. C. Mullick Road, Jadavpur, Kolkata-700032.India*
+91 33 24838083, Fax:+91 33 24730957
* *skbhadra@cgcri.res.in*

We study the birefringence property of suspended core (SC) photonic crystal fibers (PCF) selectively filled with metal wires in the first ring of air holes of the claddings. The structures of three drawn suspended solid-core PCFs are analyzed by using mode solver of COMSOL Multiphysics based on finite element method (FEM). Numerical simulation shows that birefringence of the order of 10^{-3} can be achieved by filling two consecutive air holes of the first ring of the photonic crystal cladding with metal wires.

So far various highly birefringence solid-core [1, 2] as well as hollow-core [3] PCFs have been reported. In these reported fibers birefringence is achieved by introducing asymmetries into the fiber core or cladding. However the degree of birefringence can be further increased by selectively filling the air holes of specially designed PCFs with metal wire. Several theoretical and experimental studies show that polarization dependant coupling of surface plasmon (SP) mode with core guided mode is possible [4, 5]. In this study the polarization dependant coupling of SP mode with the core guided mode is utilized to obtain high birefringence.

The cross section of the drawn SC PCF is shown in Fig 1 (a). This structure is redrawn with silver wires (dark circles in Fig 1 (b)) in the cladding and analyzed by using FEM. The effective refractive indices of the horizontal (n_x) and vertical (n_y) polarisation are used to obtain the modal birefringence $n_x - n_y$ and the variation of modal birefringence is shown in Fig 1. (d).

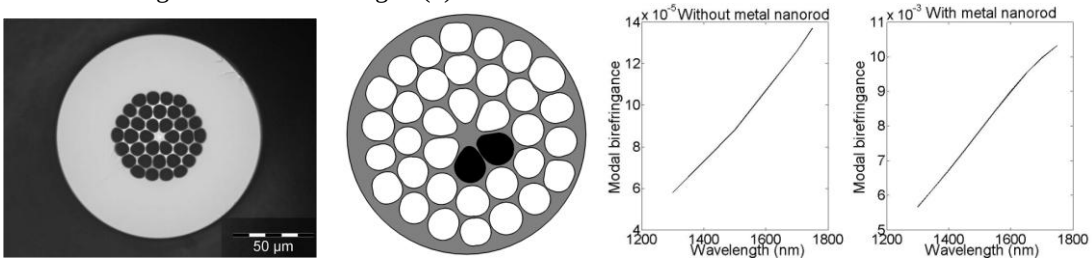

(a) (b) (c) (d)

Fig 1: (a) Drawn SC PCF with suspension factor SF =1.45. (b) Schematic diagram of the same fiber with metal wires (dark circles) in the claddings. (c) Variation of modal birefringence with wavelengths of structure (a). (d) Variation of modal birefringence with wavelengths of structure (b).

The modal birefringence plots show that the degree of birefringence can be increased at the order of 10^2 by filling two consecutive air holes with silver wires. The fiber has 2.4 times higher birefringence than the fiber having metal wires with perfectly circular air holes.

Acknowledgement: The authors would like to acknowledge, Director, CSIR-CGCRI for support and encouragement to carry out this work.

References:

[1] A. Ortigosa-Blanch, J. C. Knight, W. J. Wadsworth, J. Arriaga, B. J.Mangan, T. A. Birks, and P. St. J. Russell, *Opt. Lett.*, **25**, 1325 (2000).
[2] T. P. Hansen, J. Broeng, S. E. B. Libori, E. Knuders, A. Bjarklev, J. R.Jensen, and H. Simonsen, *IEEE Photon. Technol. Lett.*, **13**,588 (2001).
[3] K. Saitoh and M. Koshiba, *IEEE Photon. Technol. Lett.*, **14**, 1291 (2002).
[4] H. W. Lee,M. A. Schmidt,H. K. Tyagi,1 L. P. Sempere, and P. S. J. Russell, *Appl. Phys. Lett*, **93**,111102 (2008).
[5] A. Nagasaki, K. Saitoh, and M. Koshiba, *Opt. Express.***19**, 3799(2011).

Embedding multiple non-diffracting defect sites in 2D photonic lattice by optical phase engineering

Manish Kumar[a,*] and Joby Joseph[a]
[a] *Photonics Research Lab, Department of Physics, Indian Institute of Technology Delhi, Hauz Khas, New Delhi, India - 110016*
* *manishk@physics.iitd.ac.in*

Multiple beam interference based lithographic methods have enabled single step, large area micro-fabrication of periodic structures in photo-sensitive media. These periodic structures are referred to as photonic crystals which have the feature size of the range of the wavelength of light and are capable of modifying the light propagation characteristics leading to a wide range of applications. The light propagation characteristics here depend on the photonic band-diagram of these structures. Just like their electronic counterparts, namely semiconductors, these photonic crystals exhibit band-gaps known as photonic band-gap in which no photon is allowed to propagate through the crystal [1]. Adding an artificial defect site in these otherwise periodic structures opens up new possibilities by creating a channel in the band-gap region that leads to light confinement for cavity, lasing, sensing and other applications. But introduction of non-diffracting (ND) defect site in 2D periodic lattice had not been explored until recently when zero order Bessel beam was superimposed with periodic lattice wave-field of 3 beam interference [2]. This technique has been extended to introduction of ND defect site in spiralling lattice wave-field as well [3]. The main advantage of this method is single step fabrication of lattice with defect sites where one need not worry about precise positioning of recording media due to ND characteristics of resultant beam.

In present work, we show that this method of combining Bessel beam with periodic lattice wave-field could be used to embed multiple defect sites at desired positions in 2D photonic lattice structure. As an example we take hexagonal lattice formed by three beam interference and add multiple Bessel beams coherently to it, where each Bessel beam is centred at corresponding defect site. The phase part of resultant field is extracted and displayed on a phase only SLM. A simple 4-f setup based Fourier filtering is applied to get the resultant defect embedded lattice in the imaging plane.

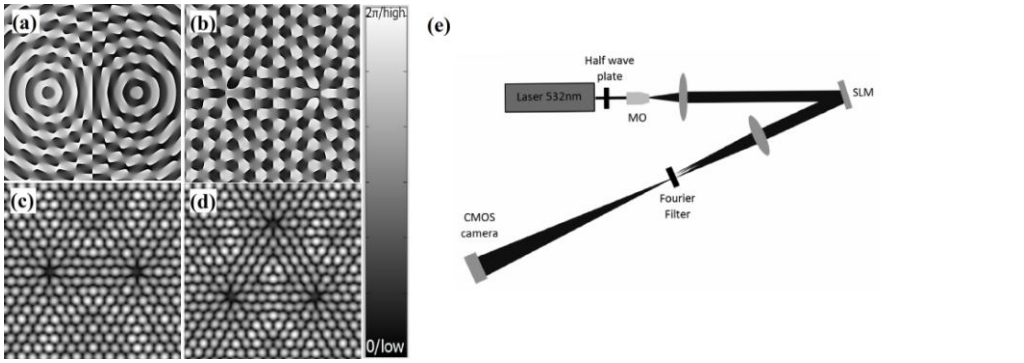

Fig. 1: Embedding multiple defect sites in hexagonal lattice by phase engineering. (a) Phase part of sum of two off-cantered Bessel beams. (b) Sum of hexagonal lattice field and two Bessel beams from (a). (c) Resultant intensity profile for two embedded defects due to corresponding phase shown in (b). (d) Resultant intensity profile for 3 embedded defects in hexagonal lattice (corresponding phase not shown). Colorbar represents phase variation 0-2π Or, intensity variation low to high. (e) Schematic of the experimental setup.

References:

[1] J. D. Joannopoulos, S. G. Johnson, J. N. Winn, and R. D. Meade, "Photonic crystals: Molding the flow of light" Princeton university press, 2011.
[2] A. Kelberer, M. Boguslawski, P. Rose, and C. Denz, "Embedding defect sites into hexagonal non-diffracting wave fields," *Opt. Lett.* **37**, 5009–5011 (2012).
[3] M. Kumar, and J. Joseph, "Embedding a nondiffracting defect site in helical lattice wave-field by optical phase engineering" *App. Opt.* **52** (2013) (Accepted)

Dual Band Cross Polarization Converter Formed by V-Shaped Chiral Metamaterial

R. Rajkumar, N. Yogesh, S. Lincy and V. Subramanian*
[a] *Microwave Laboratory, Department of Physics, Indian Institute of Technology Madras, Chennai-600 036, India.*
* manianvs@iitm.ac.in

A dual narrow band cross polarization converter formed by V-shaped chiral metamaterial (VSCMM) having more than 90% polarization conversion efficiency is demonstrated numerically [1]. The giant optical activity in the proposed VSCMM arises due to the strong cross-coupling between the electric and magnetic fields. The mechanism of coupling is explained based on the surface current distribution on the top and bottom metallic structure of VSCMM [2]. The proposed bilayered VSCMM has C_4 rotational symmetry of an enantiomeric pattern and it lacks the mirror symmetry in the direction of wave propagation which provides the optical activity for realizing the cross polarization conversion [3].

Figure 1(a) shows the numerical results (using CST Microwave Studio) of cross (T_{xy}, where y is the incident direction and x is the receiving direction) and co polarization (T_{yy}) transmission coefficients of the VSCMM. At 15.675 GHz and 23.985 GHz, maximum cross polarization efficiency (CPE) of 95% and 91% is observed respectively. At 15.675 GHz, anti-symmetric currents (Fig. 1(b)) provides strong magnetic coupling for the incident electric field along *y* direction. On the other hand, at 23.985 GHz, dominant electric dipole coupling (Fig. 1(c)) shows chiral response. In both the cases, due to the asymmetric geometry of the proposed VSRR, observed resonances gives rise to a strong chirality so that the polarization plane of the incident e-m wave is rotated at a large angle while propagating through the chiral medium [4-5]. The presence of the four-fold rotational symmetry and the reciprocity in the metamaterial structure, allows only the symmetric linear polarization conversion of the incident wave. The proposed dual band VSCMM cross polarization converter is anticipated for the efficient polarizing element in microwave/optical polarization spectroscopy and microwave photonics applications.

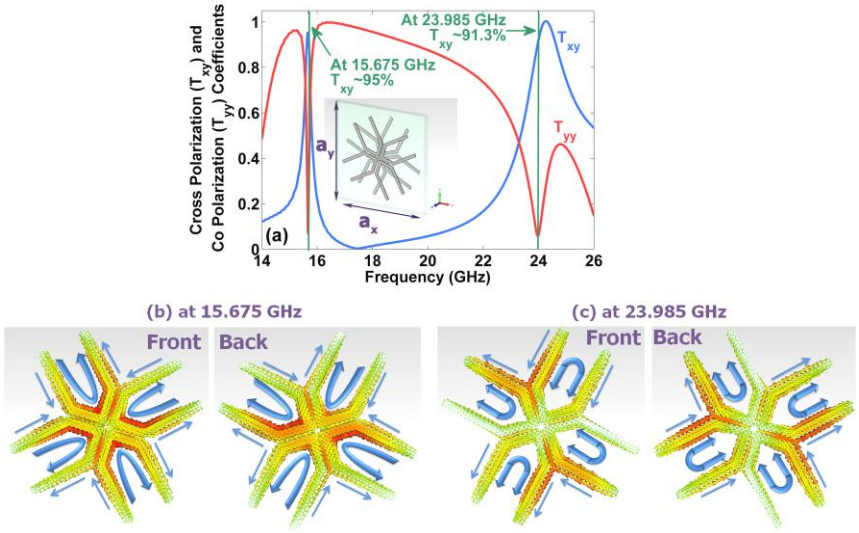

Fig.1(a) Cross polarization coefficient T_{xy} at 15.675 GHz and 23.985 GHz.(inset VSCMM unit cell), (b) and (c) show the surface current distribution on top and bottom metallic patterns of VSCMM at 15.675 GHz and 23.985 GHz respectively.

References:

[1] Y. Ye and S. He, *Appl. Phys. Lett.*, **96**, 203501 (2010).
[2] J. Shi, X. Liu, S. Yu, T. Lv, Z. Zhu, H. F. Ma and T. J. Cui, *Appl. Phys. Lett.*, **102**, 191905 (2013)
[3] R. Zhao, L. Zhang, J. Zhou, Th. Koschny and C. M. Soukoulis, *Phys. Rev. B.*, **83**, 035105 (2011)
[4] A. Papakostas, A. Potts, D. M. Bagnall, S. L. Prosvirnin, H. J. Coles and N. I. Zheludev, *Phys. Rev. Lett.*, **90**, 107404 (2003)
[5]K. Song, Y. Liu, Q. Fu, X. Zhao, C. Luo and W. Zhu, *Opt. Exp.*, **21**, 7439 (2013).

Threshold features of photonic-crystal heterostructure lasers

M. Srinivas Reddy,[a,*] Ramarao Vijaya,[b] Ivan D. Rukhlenko,[c] and Malin Premaratne[c]
[a]*IITB-Monash Research Academy, CSE Building 2nd Floor, IIT Bombay, Powai, Mumbai 400076, India*
[b]*Department of Physics, Indian Institute of Technology Kanpur, Kanpur 208016, India*
[c]*Advanced Computing and Simulation Laboratory (AχL), Department of Electrical and Computer Systems Engineering, Monash University, Clayton, Victoria 3800, Australia*
** cnu.munige@gmail.com*

Low-threshold lasing from a photonic crystal (PhC) can be achieved either by creating a defect [1] or by reducing the group velocity near the band edges [2]. We have theoretically analyzed [3] and experimentally demonstrated [4] lasing near the first-order band edge of a dye-doped PhC. Here, we propose and analyze a heterostructure-based laser cavity, in which a decrease in the lasing threshold is achieved by combining a defect layer design with the tailored low group velocity range of frequencies.

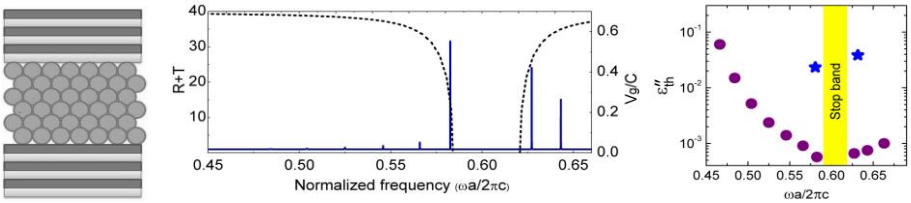

Fig. 1. (a) Schematic of proposed heterostructure PhC cavity, (b) sum of reflection and transmission (R+T) in arbitrary units as a function of frequency for heterostructure PhC cavity, calculated by assuming a complex-valued permittivity with ε″=0.0005 for the dielectric spheres of the sandwiched 3D PhC while the calculated group velocity is shown as dashed curve, and (c) the lasing threshold for cavity modes (filled circles) of proposed structure and the frequencies near the band edges for the stand-alone 3D PhC (stars).

Schematic of the proposed heterostructure PhC cavity can be seen in Fig. 1(a). It is composed of an active three-dimensional (3D) PhC sandwiched between two identical passive multilayer stacks. We calculated its lasing threshold characteristics using Korringa-Kohn-Rostoker method [5]. Assuming that the gain medium is uniformly doped in the building blocks of the PhC, the gain can be modeled using complex-valued permittivity $\varepsilon=\varepsilon'-i\varepsilon''$ ($\varepsilon'' > 0$). In the calculations, we assume that the 3D PhC with lattice constant *a*, is made of polystyrene spheres ($\varepsilon'=2.53$) doped with gain medium. The multilayers are composed of 5 double layers each, with $\varepsilon_1=7.02$ (TiO_2), $\varepsilon_2=2.37$ (SiO_2) and thicknesses $t_1=0.25a$ and $t_2=0.16\,a$, respectively. We chose the period and the permittivity of the multilayer in such a way that its stopband is broad enough to cover the stopband of the sandwiched 3D PhC. The divergence in the calculated sum of reflectance and transmittance (R+T) as a function of frequency for the cavity modes (seen in Fig. 1(b)) can be attributed to lasing oscillations [2]. ε_{th}'' which serves as a measure of lasing threshold is that value at which R diverges logarithmically. The divergence points (filled circles) for heterostructure PhC cavity modes are given in Fig.1 (c). The lasing threshold is lowered as the mode approaches the band edges of the sandwiched 3D PhC. The star symbols indicate the lasing threshold for a stand-alone 3D PhC. A decrease of two orders of magnitude in the lasing threshold is obtained for the heterostructure PhC cavity as compared to a stand-alone 3D PhC. We also present a dependency of threshold gain on number of layers in the multilayer as well as in sandwiched 3D PhC.

Acknowledgement:
MSR gratefully acknowledges Prof. S. Dhar at the Department of Physics, IIT Bombay, for mentorship. The work of RV was supported by the, Instrument Research and Development Establishment, Dehradun, India under the DRDO Nanophotonics program (ST-12/IRD-124). RV acknowledges Director of IRDE for granting the permission to publish this work. The work of IDR and MP is supported by the Australian Research Council, through its Discovery Early Career Researcher Award DE120100055 and Discovery Grant DP110100713, respectively.

References:

[1] S. John, *Phys. Rev. Lett.* **58**, 2486 (1987).
[2] K. Sakoda, K. Ohtaka, and T. Ueta, *Opt. Express* **4**, 481 (1999).
[3] M. S. Reddy, R. Vijaya, I. D. Rukhlenko, and M. Premaratne, *Opt. Lett.* **38**, 1046 (2013).
[4] M. S. Reddy, S. Kedia, R. Vijaya, A. K. Ray, S. Sinha, I. D. Rukhlenko, and M. Premaratne, *IEEE Photonics J.* **5**, 4700409 (2013).
[5] N. Stefanou, V. Yannopapas, and A. Modinos, *Comput. Phys. Commun.* **113**, 49 (1998).

Directional Multi-Beam Antenna and Electromagnetic Energy Concentrator Using Photonic Crystals

N. Yogesh, and V. Subramanian*
Microwave Laboratory, Department of Physics, Indian Institute of Technology Madras, Chennai-600036, INDIA.
* manianvs@iitm.ac.in

Maxwell's equations are form invariant under coordinate transformation (CT) [1]. This fact implies the way to obtain new trajectories for the electromagnetic (e-m) wave as CT scales the constitutive parameters (dielectric permittivity and magnetic permeability) of the e-m space. For example, an e-m source kept at the focal plane of a convex lens transforms a cylindrical wavefront in to a plane wavefront. However, this cannot be implemented in the integrated devices owing to the miniaturization. CT provides an elegant method for source transformation, where a cylindrical wavefront in an air medium is mapped on to an e-m space with a plane wavefront [2]. The mapped e-m space can be designed using metamaterials whose constitutive parameters can be tailored from positive to negative values. This concept of source transformation is warranted for optical communication, microwave photonics, nanophotonic devices and optical antennas in biosensing applications. Nevertheless, metamaterials barely fulfill the requirements due to metallic losses, scalability and requirement of intricate design procedure. On the other hand, photonic crystal (PCs) made up of periodic dielectric constitutions can serve as another avenue, where the multi-beam transformation is scalable to all e-m frequencies.

The multi-beam transformation in PCs relies on the behavior of e-m wave at near-band gap (NBG) frequencies rather than CT method [3]. It is known that the e-m wave at NBG frequencies in PCs is neither a standing wave nor a traveling wave, rather it takes a form of slowly varying envelope (SVE) profile irrespective of the nature of an incident source (cylindrical or planewave source). This nature is explored to design a directional multi-beam antenna as Fig.1(a) shows the four-beam transformation in a PC cavity formed by prism wedges made of one-dimensional periodic dielectrics (air of thickness 0.5*a* and glass of dielectric constant 5.5 with a thickness of 0.5*a*, where *a* is the lattice constant). E_z profile at 10.8 GHz shown in Fig. 1(a) demonstrates the transformation of a cylindrical wavefront emitted by a monopole at the center of the cavity in to directional four beams at the output. The computed directionality of the photonic four-beam antenna is around 15 dBi.

Suppose, if one think of the reverse situation, where a PC cavity is excited with multiple beams, one can expect the energy concentration due to e-m wave trapping at the center of the cavity as shown in Fig. 1(b). In this case, PC cavity will be useful for e-m energy harvesting. For instance, mobile phone communication frequency band (800 MHz to 2 GHz) is presented everywhere. Storing this microwave energy within a small space can be useful for an efficient microwave heating. By optimizing the cavity for the random phase of the incident fields, one may realize an efficient energy harvesting device.

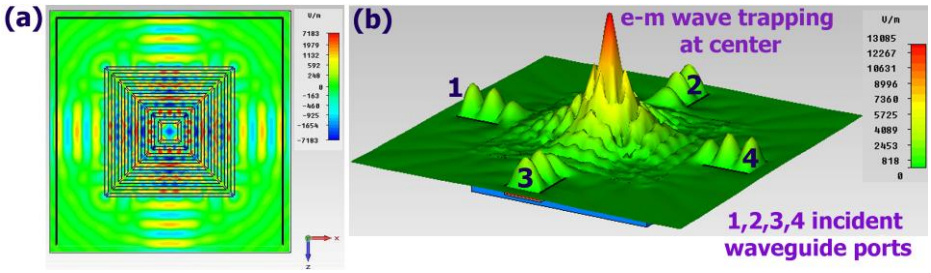

Fig.1(a) Four-beam antenna E_z at 10.8 GHz. (b) Wave storage in PC cavity (alumina-0.3*a*), E_z-12.26 GHz.

References:

[1] J. B. Pendry, D. Schurig, and D. R. Smith, *Science*, **312**, 1780 (2006).
[2] J. P. Turpin, A. T. Massoud, Z. H. Jiang, P. L. Werner, and D. H. Werner, *Opt. Exp.*, **18**, 244 (2010).
[3] N. Yogesh and V. Subramanian, *Opt. Lett.*, **36**, 1737 (2011).

Slow light effects in photonic crystals

Ummer K.V.* and R.Vijaya
Department of Physics, Indian Institute of Technology Kanpur, Kanpur 208016, India
** ummerkv@iitk.ac.in*

Photonic crystals are periodic dielectric structures whose periodicity determines the wavelength range of their operation and application. As a result of their interesting band structures, the group velocity of the modes at the edges of Brillouin zone boundaries are tremendously lowered, thus offering the possibility of various slow light effects in them. The control of optical signals in the time domain enables the compression of their energy in space, leading to reduced device footprints and enhancement of light matter interaction [1]. The lowered group velocity also offers an enhancement of nonlinear effects and optical gain. In this work, the possibility of slow light effects in photonic crystals is explored by calculating the band structure as well as the associated group velocities and group indices of the bands.

The band diagram of a three-dimensional (3-D) photonic crystal with face centred cubic (*fcc*) lattice arrangement and the corresponding group velocity ($v_g = d\omega/dk$) in units of v_g/c and group index (n_g) are calculated using the BandSOLVE module of RSoft^{TM}. The group index is calculated as $n_g = n + \omega_1\, dn/d\omega_1$ [1], where the effective refractive index (n) and the eigen frequencies of the modes (ω_1) are available from the simulations. In Fig. 1(a), one can notice different regimes. The group velocity has a constant value in the long wavelength regime, where the projected density of states along the propagation direction is equal to the density of states of the bulk medium. In the slow light regime, relevant at k points near the centre or the edges of the Brillouin zone, the group velocity is reduced due to the Bragg diffraction [2] and the group index (not shown here) is increased. The superluminal regime is relevant for frequencies within the band gap [3]. a is the lattice constant and k is the wave vector.

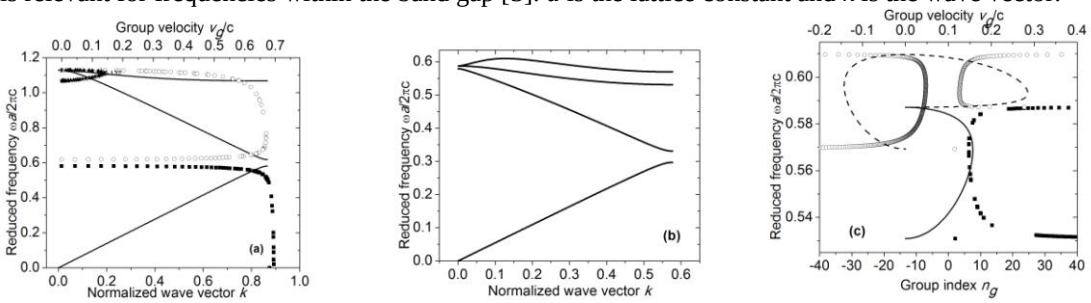

Fig.1(a) Band diagram (solid line) and group velocity (square, circle and star symbols) for the first three bands of the 3-D *fcc* structure (with an index contrast of 0.6) along the ΓL direction, (b) the first 4 bands of 2-D hexagonal structure for TE polarization along the ΓM direction and (c) the group index (square and circle symbols) and group velocity (solid and dashed line) of the third and fourth bands of Fig. 1(b).

In Fig.1 (b), the first four bands of the band structure are shown for a 2-D hexagonal structure consisting of circular holes of radius r in a solid dielectric slab of index 2. For this calculation, r/a is chosen to be 0.25. The corresponding group velocity and group index are shown for the third and fourth bands in Fig.1(c). The group velocity is lowered at the band edges as seen earlier for the 3-D structure, and the associated group index is increased as expected. However, the extremum of the fourth band at $k = 0.128$ has zero group velocity. This point is neither a zone centre nor a zone edge. The extrema can happen due to the avoided eigen value crossing or band repulsion [2]. In addition, the presence of positive and negative values of group index for the fourth band shows that the medium can behave as left-handed or right-handed depending on whether the group velocity and phase velocity are anti-parallel or parallel to each other in this frequency range [2].

The work of RV is supported by the Instrument Research and Development Establishment, Dehradun, India under the DRDO Nanophotonics program (ST-12/IRD-124). RV acknowledges the Director of IRDE for granting the permission to publish this work.

References:

[1] Toshihiko Baba, N*ature Photonics*, **2,** 465 (2008)
[2] M. Ghebrebrhan, M.Ibanescu, S.G.Johnson, M.Soljacic and J.D.Joannopoulos, *Phys. Rev.* A **76**, 063810 (2007)
[3] Jesper Goor Pedersen, S.Xiao and N.A.Mortensen, *Phys. Rev.* B **78**, 153101 (2008)

Design of helical metamaterial based broadband circular polarizer with improved extinction ratio for VIS-NIR optical region

Saraswati Behera[a], Joby Joseph[a]

[a] *Photonics Research Lab., Department of Physics, Indian Institute of Technology, Delhi, Hauz Khas, New Delh-110016*

joby@physics.iitd.ac.in

The artificially designed materials known as metamaterials have come up now-a-days with wide applications in manipulating and controlling the light as well as sound, which are unachievable with the naturally occurring materials. Advances in nano-technology have revealed compact and robust devices based on these metamaterials. Broadband optical circular polarizer based on helical metamaterial structure is of current interest [1] such structures show giant optical activity and circular dichroism, hence has applications in spectrometers, life science microscopy, and display devices. Though broad operation band is achieved by different research groups, with tapered helical structures [2] as well as double and multi-helical structures [3], improvement in the optical performance of such structures is still a challenge. The extinction ratio has also been improved to 83:1, OB=0.58 to 1.36 μm with conical double helix structures by Zhao et.al. [4]. If one look towards improved optical performances in broad OB, the design of structure becomes more complex. In the present work we have emphasized more towards improving the optical performance of simpler structures rather than complex structures.

We have designed helical metamaterial structure based on the finite difference time domain simulation. The structure is optimized for the aluminium single helical left-handed structure with the parameters: periodicity (a) = 200 nm, length of each pitch of helix (L) = 400nm, number of pitches in the helix (N) = 4, Diameter of helix (D) = 100 nm, diameter of the wire of the helix (d) = 60nm. Material of the helix is aluminium (Al) whose refractive index is defined by Drude-Lorenz model for metals. The refractive index of the substrate is 1.45. Circularly polarized (RCP and LCP) light is incident normally along the backward z axis. As the helix is oriented along clockwise (left-handed), the RCP light is expected to be transmitted and the LCP should be completely reflected. But the material loss (absorption) and small size of the helix (finite end point) limits the optical performance. Hence our present study aims at increasing the average extinction ratio of the single helical structure over a broad operation band by optimizing various structure parameters. We have achieved AER 97:1 in the VIS-NIR (586-968 nm) OB region with average transmittance of 74% for the RCP light. OB= Operation Band (wavelength region on which the average extinction ratio is above 10dB), AER= Average Extinction Ratio = T (RCP) / T (LCP)

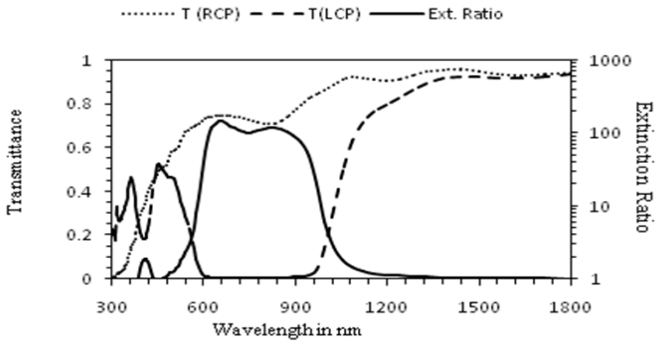

Figure 1. *Optical performance of optimized aluminium handed structure simulated by FDTD*

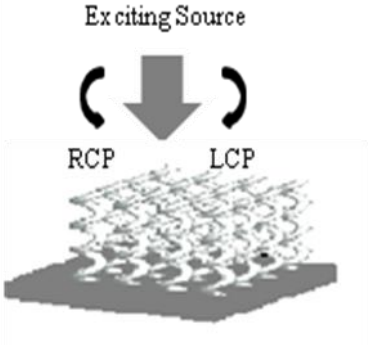

Figure 2. *Modelling of the single single helical left helical structure with excitation source*

References:

[1] J. K. Gansel, M Thiel, M. S. Rill, M Decker, K Bade, V Saile, G V. Freymann S. Linde and M. Wegener *SCIENCE,* 325 (2009)

[2]J. K. Gansel, M. Latezel, A Frolich, J. Kaschke, M. Thiel and M. Wegener, *Ap. Physics Letters* 100, 101109 (2012)

[3] Z. Yang, P. Zhang, P. Xie, L. Wu, Z. Lu, M. Zhao, *Front. Optoelectron.*, 5, 248 (2012)

[4] Z. Zhao, D. Gao, C. Bao, X. Zhou, T. Lu, and L. Chen *Journal of Light wave technology* 30, 15 (2012)

Patterned sculptured thin films and photonic applications

Jhuma Dutta[a,*], S.A.Ramakrishna[a,] A.Lakhtakia[b], I. Mekkaoui Alaoui[c]

[a]*Department of Physics, Indian Institute of Technology Kanpur, Kanpur 208016, India*

[b]*Department of Engineering Science and Mechanics, Pennsylvania State University, University Park,Pennsylvania 16802, USA*

[c]*Physics Department, Cadi Ayyad University, Faculty of Sciences Semlalia, Morocco*

** jhuma@iitk.ac.in*

By collimating the vapour flux of Calcium fluoride (CaF_2) obliquely towards the lithographically fabricated micrometer/ submicrometer grating, a new kind of periodically patterned columnar thin films (PP-CTFs) has been fabricated. PP-CTFs function like blazed diffraction grating with asymmetric diffraction efficiency in transmission at ultraviolet-visible wavelengths. Triangular prismatic air cavities were periodically formed by merging the growth of diverging columnar structures of CaF_2 within the fabricated structure by controlling the various deposition parameters of vapour flux. Using Kirchhoff-Fresnel diffraction theory, it is possible to explain the blazing effect arises as a result of spatially linear phase shifts caused by the prismatic air cavities. The intensities of the diffracted order depends quite sensitively on the effective permittivity tensor of the CTFs, which in turn depends on the porosity of the film. Because of different refractive indices for two polarizations , the calculated and measured diffraction efficiencies of PP-CTFs for s and p polarized light are different. The principal refractive indices of the deposited CTFs are estimated from the diffraction efficiencies.

Visualization of latent fingerprints is enhanced by deposition of columnar thin films at large oblique angle of CaF_2 and silica (SiO_2) on fingerprint marks on two nonporous surfaces such as smooth glass slides and highly reflecting rough aluminium sheets. The vapour flux gets shadowed by the physical residues left behind in the fingerprint and preferentially gets deposited on these residues. The deposited CTFs are highly scattering and results in an enhanced visibility of fingerprint. The visualization can be further enhanced by treating the deposited CTFs with a fluorescent dye and fluorescence imaging. A specific amino-acid reagent (1,2-indanedione+alanine) and non-specific laser dye (Rhodamine 6G) are shown to help to enhance the visualization of the deposited CTFs due to the localization and entrenchment of the dye within the CTF regions.

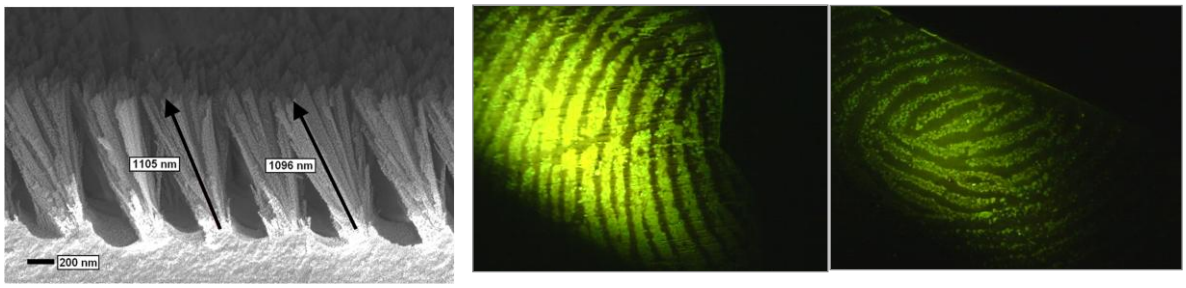

(a) **(b)**

Fig. (a) Cross sectional SEM image of PP-CTF of thickness 1100 nm deposited on a 1D photoresist grating of 600 nm period. (b) Fluorescence images of fingerprint marks with SiO_2 CTF and Rhodamine 6G treatment on a rough aluminum sheet (left-side) and a glass slide (right-side) respectively.

References:

[1] A.lakhtakia and R.Messier, SPIE Press, Bellingham, (2005)

[2] J.Dutta, S.A.Ramakrishna and A.Lakhtakia, Appl.Phys.Lett, (2013).

[3] J.Dutta, S.A.Ramakrishna and I.Makkaoui Alaoui, Forensic Science International (2013).

Modification of line shape of an amplifying medium induced by surface plasmons

Prince Gupta* and S. Anantha Ramakrishna
Department of Physics, Indian Institute of Technology Kanpur, Kanpur-208016, India
* *gprince@iitk.ac.in*

Plasmonics offers an effective future for the device development as it has both large bandwidth of photonics and possibility of miniaturization of electronics [1]. But the dissipation of surface plasmons within few micrometers of propagation hinders the applications in wide range device technology [2]. Surface plasmon resonances are also important in realizing Metamaterials at high frequencies [3]. Since at high frequencies metal start behaving as plasma,the inherent plasmonic losses once again limits the application of Metamaterials.

This inherent loss present in surface plasmon can be compensated by introducing active gain medium [4]. The interaction of intense radiation field of surface plasmon with active gain medium not only influences the transition rates between the states of the active medium, but also influences the level structure. The change of the structure (splitting of levels) arises due to strong field enhancements due to the resonance excitement of the surface plasmons. The interaction of the surface Plasmon resonance with the level resonance of the active medium gives rise to a rich dynamics and level anticrossings.

In this poster, we report the modification of the line shape of an amplifying medium induced by local electric field of surface plasmon at resonance and compensation of the loss for surface plasmon resonance by amplification on gold corrugated grating by laser pumped Rhodamine-6G. An experimental demonstration of the modification of surface plasmon resonance dip by varying pump power in presence of amplifying medium is presented.

.

References:

[1] E. Ozbay, *Science*. ***311***, 189-193 (2006).
[2] S. A. Maier, **Springer** (2007).
[3] S. Anantha Ramakrishna and Tomasz M. Grzegorczyk, **421 pages**, CRC Press, Boca Raton (2009)
[4] J. Seidel, S. Grafstrom, and L. Eng, Phys. Rev. Lett., **94**,177401(2005).

Analysis of Two Dimensional Graded Photonic Crystals towards Negative Index Medium

Praveen C Pandey* and V. Vidhya Lakshmi
Department of Applied Physics, Indian Institute of Technology
(Banaras Hindu University), Varanasi-221005 (UP), INDIA
* Corresponding author- Tel.: +91 5426702008; fax: +91 542 2368428.
E-mail address: pcpandey.app@itbhu.ac.in (Praveen C Pandey).

Abstract:

The band structure of two dimensional photonic crystals is analyzed using Plane wave expansion and FDTD techniques. Ordinary 2-D triangular lattices and graded photonic crystals (GPCs) have been simulated to realize an effective negative refractive index. In ordinary 2-D photonic crystals (PCs), structures are composed of dielectric columns in a triangular lattice fashion along normal to the incident wave. We then study, how the photonic band gap and response of wave in our structures is affected by changing radii of the dielectric rods. We observed that response of wave in 2-D triangular PC structure is highly depending on the radii of rods as shown in figure (1).

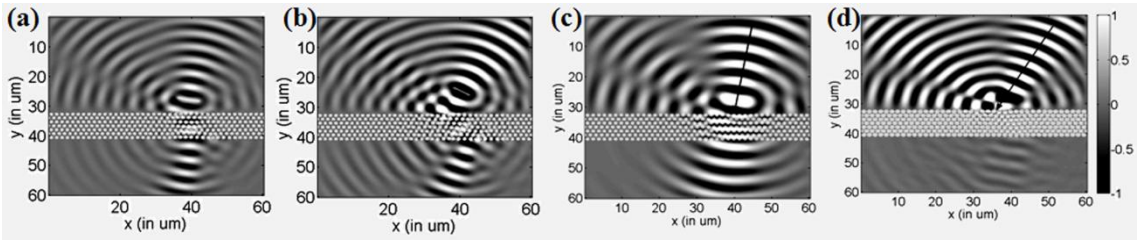

Figure 1: Response of the 2D triangular PBG structure to a Gaussian beam for different radii of dielectric rod (a) & (b) for r=0.35a and (c) & (d) for r = 0.455a of incident at 10° and 30° to the normal, respectively.

The 2-D GPCs are composed of dielectric rod with graded radii or refractive index along the direction transverse to the propagation. By controlling the gradient of the refractive index and radii of the dielectric rods, it is possible to obtain either a focusing lens with Fourier transforming capability or an imaging lens, which produced inverted images. Figure 2 shows the propagation of electric field in 2-D GPC with graded radii of dielectric rod for different radii surface.

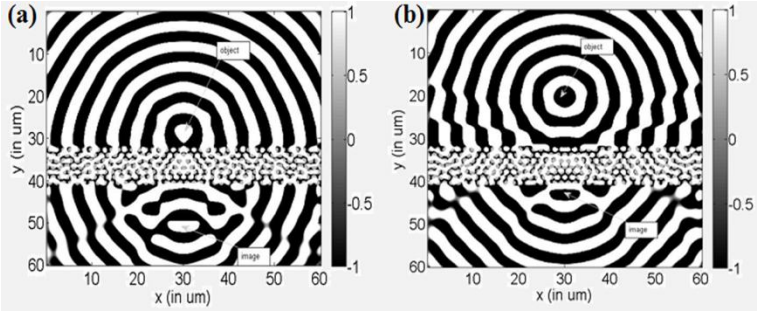

Figure 2: Propagation map of electric field in GPC for source (object) at (a) 2a & (b) 7.25a from the GPC surface.

Theses GPCs based designe can be utilized as super lens and super bending.

Improvement in Scanning Performance of Linear Printed Array Antenna Integrated with Uniplanar Compact EBG (UC-EBG) Structure

Pratik Mevada, Sanjeev Kulshrestha, Dr. S. B. Chakrabarty and Rajeev Jyoti
Microwave Sensors Antenna Division, Space Applications Centre (SAC), Indian Space Reasearch Organization (ISRO), Ahmedabad, India

Abstract — In scanning array antennas, surface wave coupling between inter-elements of array plays major role in limiting antenna scanning range. Mutual coupling of these surface wave modes cause scan blindness at an angle resulting into restricted range of antenna scanning. In order to eradicate scan blindness, stop-band characteristics of electromagnetic band-gap structures has to be performed. Therefore, this paper presents analytically based approach for the design of 16 element linear printed array antenna integrated with Uniplanar Compact Electromagnetic Band Gap (UC-EBG) Structure. Analysis and simulation of Active Reflection Coefficient (ARC) and Active Radiation Pattern (ARP) is also presented to demonstrate scan blindness removal. The design is validated by observing the simulated gain variation of the radiation pattern at scanned angle. Simulations are performed using the MoM-based Ansys Designer 8.0 EM Simulator.

Index Terms — Microstrip Antenna, Uniplanar Electromagnetic Band Gap, Active Reflection Coefficient, Active Radiation Pattern.

Near field probing of the surface waves on a planar metal surface patterned with annular holes

M. Misra[1], Y. Pan[2], C. R. Williams[2], S. A. Maier[3] and S. R. Andrews[2]
[1]*Faculty of Electronics & Communication Engineering, Shri Ramswaroop Memorial University, Lucknow- Deva Road, Barabanki 225003, India*
[2]*Department of Physics, University of Bath, Bath BA2 &AY, UK*
[3] *Department of Physics, Imperial College London, London SW7 2AZ,UK*
[*]*mukul.ec@srmu.ac.in*

We have performed the near field probing of the surface waves on a planar metal surface patterned with annular holes by photoconductive THz near field probe [1]. We have designed and fabricated the above mentioned micro-structured surface to guide surface waves which mimick SPPs. Electron micrographs of the structure, whose far field properties have been described previously [2], are shown in Fig. 1 (a,b). It consists of a 60 μm thick sheet of patterned and cured epoxy based SU-8 photoresist, conformally coated with copper and supported on a 500 μm thick pyrex substrate. The high aspect ratio pattern consists of a square □ =80 μm period array of h=50 μm deep annular recesses with inner radius a_{in}=10 μm and outer radius a_{out}=30 μm. It supports a TEM-like mode (~1.1THz) bound to the central pillar and a TE_{11}-like mode (~1.79 THz) localized at the edge of the hole. The surface waves were experimentally studied in the near field. Radiation was end-fire coupled into the guided modes of the 40 mm long, 6 mm wide structure using a cylindrical silicon lens and detected with a 10 μm dipole probe with integrated 20 μm aperture as shown in Fig.1(c).

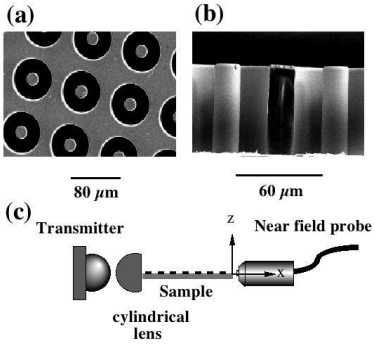

Fig. 1: (a) Electron micrograph of top surface of the metamaterial waveguide. **(b)** Cross section of the guide showing vertical side walls. **(c)** Schematic of end-fire coupling and near field probing arrangement and

Fig.2a shows an intensity map of time domain traces obtained at different heights z above the sample surface and a distance x=40 μm beyond the end of the sample. To a first approximation this can be viewed as a map of the z component of the electric field at the point of launching into free space. The oscillations in the time traces are associated with dual band propagation in the TEM and TE_{11} character modes described above. This is shown more clearly in the corresponding spectral map shown in Fig. 2b. A section through Fig. 2b at z=100 μm and x=40 μm calculated using the finite integration technique with a 3 THz bandwidth input pulse. The calculated spectrum for the TEM mode is narrower and shifted to higher frequency compared with experiment, probably because of slight differences between the nominal and actual structures arising from non-uniform resist thickness. The calculated spectra are not very sensitive to the exact choice of x. The ratio of the integrated areas under the TEM and TE peaks is however similar in experiment and calculation.

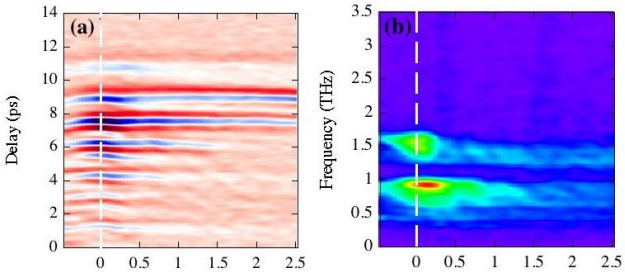

Fig. 2: **(a)** Map showing out of plane electric field versus delay at different z positions above the metamaterial surface plane and x=40 μm beyond the end of the guide. Red represents positive amplitude, blue negative and white zero. **(b)** Spectra versus z position. Blue is minimum and red is maximum amplitude. The plane of the sample

References:

[1] M. Misra, S. R. Andrews and S. A. Maier, *Appl. Phys. Lett*., **100**, 191109 (2012)
[2] C. R. Williams, M. Misra, S. R. Andrews, S. A. Maier, S. Carretero-Palacois, S. G. Rodrigo, F. J. Garcia Vidal and L. Martin-Moreno, *Appl. Phys. Lett*, **96**, 011101 (2010).